

PalArch's Journal of Archaeology of Egypt / Egyptology

MISCIBILITY STUDIES OF BIOCOMPATIBLE XANTHAN GUM/METHYLCELLULOSE BLEND-MAGHEMITE NANOCOMPOSITE

M. S. Bhavya¹, K. S. Sudhanva Narayana², P. Prasad³, M. B. Savitha⁴

¹Centre for Nano Science and Technology, College of Engineering and Technology, Srinivas University, Surathkal, Mangaluru - 574146, Karnataka, India

²Department of Nano Technology, Srinivas Institute of Technology, Merlapadavu, Mangaluru – 574143, Karnataka, India

³Department of PG Studies in Chemistry and Research Centre, Vivekanada College, Puttur - 574203, Karnataka, India

⁴Department of Chemistry and Research Centre, Sahyadri College of Engineering and Management, Sahyadri Campus, Adyar, Mangaluru – 575007, Karnataka, India Email:

⁴savitha.chem@sahyadri.edu.in

M. S. Bhavya, K. S. Sudhanva Narayana, P. Prasad, M. B. Savitha: Miscibility Studies Of Biocompatible Xanthan Gum/Methylcellulose Blend-Maghemite Nanocomposite -- Palarch's Journal Of Archaeology Of Egypt/Egyptology 17(9). ISSN 1567-214x

Keywords: Xanthan gum, MC, Maghemite, Miscibility, Polymer Blends.

ABSTRACT

Water-soluble miscible polymer blends are extensively used water purification, biomedical engineering, agriculture applications. The biopolymers used in the present study are xanthan gum (XG) which is a natural polymer and methylcellulose (MC) is a modified natural polymer. Based on refractive index, ultrasonic velocity, density, and dilute solution viscosity measurements the XG/MC blend is found to be miscible when the XG content is more than 50% in the blend. Maghemite nanoparticles were added to the blends as compatibilizers, their homogeneity and specific intermolecular hydrogen bonding was confirmed by SEM, FTIR measurements. The TGA and tensile strength measurement confirms the improved thermal properties and mechanical strength of the XG/MC blends with and without maghemite nanoparticles..

1. Introduction

Discovered in 1963 at USA's the National Center for Agricultural Utilization Research, xanthan is one of the most popular commercially produced gums. It was first derived from the bacterial action of *Xanthomonas campestris* on plants, primarily those in the cabbage family. With the advent of viscous fermentation technology in the early 1970s, this high molecular-weight polysaccharide is now produced from cornstarch. Xanthan gum (XG) is used in a variety of industrial and oil-field applications, pharmaceutical and personal care items, and processed foods. Its broad usefulness as an emulsifying, gelling, film-forming, thickening and stabilizing agent makes xanthan gum one of the most attractive products [1-5]. Methylcellulose (MC) is the simplest cellulose derivative, where methyl groups (-CH₃) substitute the hydroxyls at C-2, C-3 and/or C-6 positions of anhydro-D-glucose units. Methylcellulose is a cellulose derivative that can be prepared from the reaction of alkali-cellulose with dimethyl sulfate (DMS) or methyl chloride. It may be used as a thickener in the food industry, as a matrix for the controlled release of drugs in the pharmaceutical industry. Methylcellulose have used in food, ceramics, personal care, pharmaceuticals, biomedical, construction, adhesives, agriculture, and many other applications [6-8].

In the literature the miscibility studies of these two polymers are not available and these blends may find specific applications. The miscibility can be enhanced by the incorporation of suitable compatible agents. Maghemite is a biocompatible magnetic nanoparticle having potential applications in the biomedical field [9-13]. It is the second most common polymorph of iron oxide. The blend properties of XG and MC are intensively studied with refractive index, density, ultrasonic velocity, and dilute solution viscometry in solution state and the blend thin films were characterized by SEM, FTIR, TGA, and UTM. Further the influence of the biocompatible magnetic nanoparticle, maghemite on the blends were determined. Since xanthan gum is anionic in nature [14], we could not apply the Huggins equation to the xanthan gum in water solution, so the solution was made in 0.1 M NaCl for viscosity studies.

2. Experimental Procedure

Xanthan gum (XG) and methylcellulose (MC) were purchased from Merck, Mumbai, India, maghemite, and research-grade NaCl (Merck make) were used in this study. Blends of XG/MC of different compositions were prepared by mixing aqueous polymer solutions. Ultrasonic velocity of the blend solutions of 0.5 % (w/v) was measured at 30°C and 40°C by an interferometric technique employing an ultrasonic interferometer (Mittal Enterprises, New Delhi) at frequency 2 MHz. The densities and refractive index of the XG/MC blend solutions (0.5 % w/v) were measured at 30°C and 40°C using a specific gravity bottle and Abbe's refractometer, respectively. Stock solutions of XG and MC were prepared (0.5 % w/v) in 0.1 M NaCl. The blend stock solutions (10/90, 30/70, 50/50, 70/30, and 90/10) were prepared by stirring the mixtures at room temperature for about 45 minutes in the NaCl solution. Using the above pure

and blend stock solutions, different blend solutions (0.01, 0.02, 0.03, 0.04, 0.05, 0.06, 0.07, 0.08, 0.09 and 0.1 w/v concentrations) were prepared and viscosity measurements were done at 30°C and 40°C using an Ubbelohde suspended level viscometer. Different temperatures were maintained using a thermostat bath with a thermal stability of $\pm 0.05^\circ\text{C}$. 0.02 wt% maghemite were used for its compatibilising effect on XG/MC blends.

Thin films of the polymers and their blends, nanocomposites, and blend nanocomposites were prepared by solution casting method. SEM photographs were recorded using a JOEL (JSM 6380LA) analyzer. FTIR spectra were recorded using NICOLET AVATAR 530 spectrophotometer. Thermogravimetric analysis of the blend films was performed over the temperature range of 20 – 500°C, using Thermogravimetric analyzer (TGA Q50 V20.2 Build 27) under nitrogen environment at a scan rate of 10°C/min. Mechanical properties were measured under tensile strain with an LLYODS UK model analyzer (LR 100K) according to ASTM standards D882.

3. Results and Discussions

3.1 Refractive index measurements

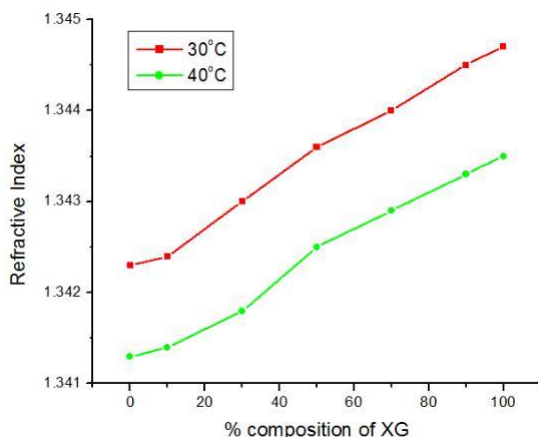


Figure 1: Variation of refractive index with the composition of XG/MC blend in aqueous solution at 30°C and 40°C

Refractive index (RI) of methylcellulose is 1.3423, and 1.3413 at 30°C and 40°C, and for xanthan gum it is 1.3447, and 1.3435, respectively. The RI value of XG/MC blends is found to be in between those of xanthan gum and methylcellulose. It is found from the graph (Figure 1) that both at 30°C and 40°C the blend compositions 50/50, 70/30, and 90/10 showed linearity with respect to XG and MC. Whereas for 10/90 and 30/70 XG/MC blends are not having linearity. The linearity indicates the miscibility/compatibility of the blends [15-17].

Due to the brownish-red color of the maghemite nanoparticle, the RI measurement technique may not be considered as a suitable proof to assess the miscibility of the blend - maghemite composites.

3.2 Density measurements

The density value of methylcellulose is found to be $0.9985 \times 10^3 \text{ Kg/m}^3$, and $0.99525 \times 10^3 \text{ Kg/m}^3$ and for xanthan gum it is $0.9999 \times 10^3 \text{ Kg/m}^3$, and $0.9966 \times 10^3 \text{ Kg/m}^3$, respectively. The density values of XG/MC blends are observed to be in between that of XG and MC but the linearity is observed for 50/50, 70/30, and 90/10 XG/MC blend compositions only at both 30°C and 40°C (Figure 2A).

With the addition of 0.02 wt% maghemite, the density value of methylcellulose is found to $0.9996 \times 10^3 \text{ Kg/m}^3$, and $0.9988 \times 10^3 \text{ Kg/m}^3$, and for xanthan gum, it is $1.0067 \times 10^3 \text{ Kg/m}^3$, and $1.0032 \times 10^3 \text{ Kg/m}^3$, respectively at 30°C and 40°C. The increase in density indicates the interaction of the polymers with maghemite. All the blend - maghemite nanocomposite compositions with 0.02 wt% maghemite showed linearity with respect to their pure polymers composites with maghemite (Figure 2B). It indicates that the incorporation of 0.02 wt% maghemite act as a compatibilizer to the blends [18].

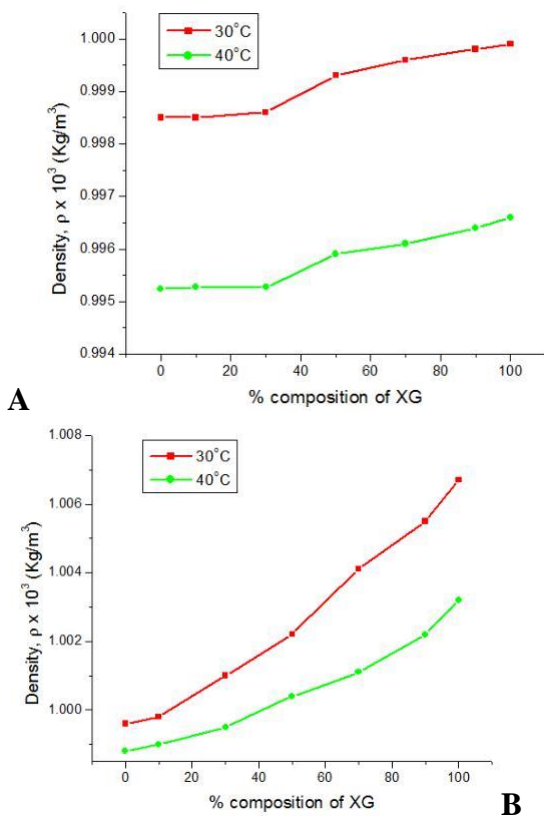


Figure 2: Variation of density with the composition of A) XG/MC blends, and B) XG/MC blend – 0.02 wt% maghemite nanocomposites in aqueous solution at 30°C and 40°C

3.3 Ultrasonic velocity measurements

The ultrasonic velocity value of methylcellulose at 30°C and 40°C is found to be 1525 m/s, and 1545 m/s and for xanthan gum it is 1473 m/s, and 1485 m/s, respectively. The ultrasonic velocity values of XG/MC blends are observed to be in between that of XG and MC but the linearity is observed for 50/50, 70/30,

and 90/10 XG/MC blend compositions only at both 30°C and 40°C (Figure 3A).

4. With the addition of 0.02 wt% maghemite, the ultrasonic velocity value of methylcellulose at 30°C and 40°C is found to be 1510 m/s, and 1524 m/s, and for xanthan gum it is 1434 m/s, and 1462 m/s, respectively. All the blend - maghemite nanocomposite compositions with 0.02 wt% maghemite showed linearity with respect to their pure polymers composites with maghemite (Figure 3B). It indicates that the incorporation of 0.02 wt% maghemite acts as a compatibilizer to the blends [19-22].

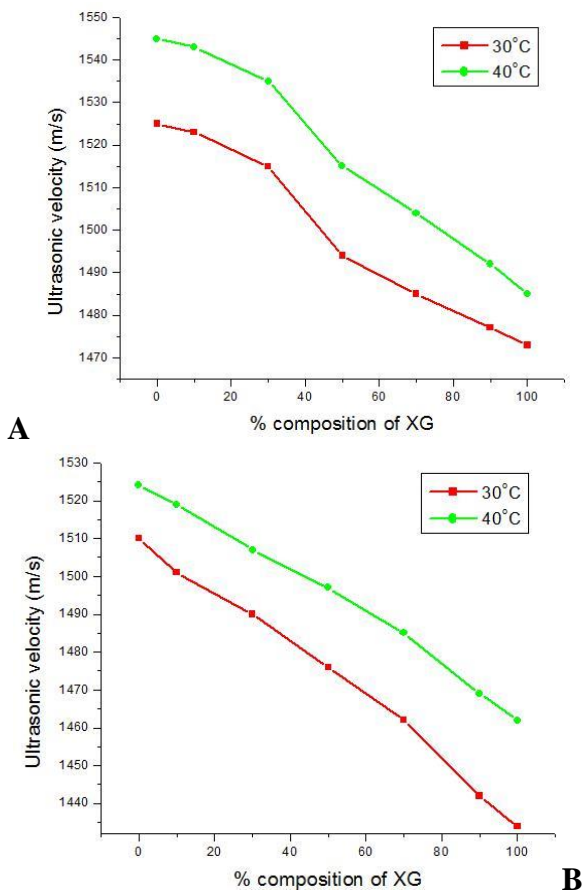


Figure 3: Variation of ultrasonic velocity with the composition of A) XG/MC blends, and B) XG/MC blend – 0.02 wt% maghemite nanocomposites in aqueous solution at 30°C and 40°C

3.4 Reduced viscosity measurements

Reduced viscosities of homopolymers XG, MC and their blend compositions (10/90, 30/70, 50/50, 30/70, and 90/10), XG – 0.02 wt % maghemite nanocomposite, MC – 0.02 wt% maghemite nanocomposite, and their blend compositions (10/90, 30/70, 50/50, 30/70, and 90/10), were measured at 30°C and 40°C. Huggin's plots of reduced viscosities against concentrations are shown in Figure 5.

At both 30°C and 40°C all the plots of XG/MC blend compositions were found to be linear. A higher slope variation is observed for 90/10, 70/30, and 50/50

XG/MC blends, whereas comparatively lower slope for 10/90, and 30/70 XG/MC blend compositions. It confirms that the XG/MC blend is miscible when XG content is 50% or more [23]. The slope values are tabulated in Table 1.

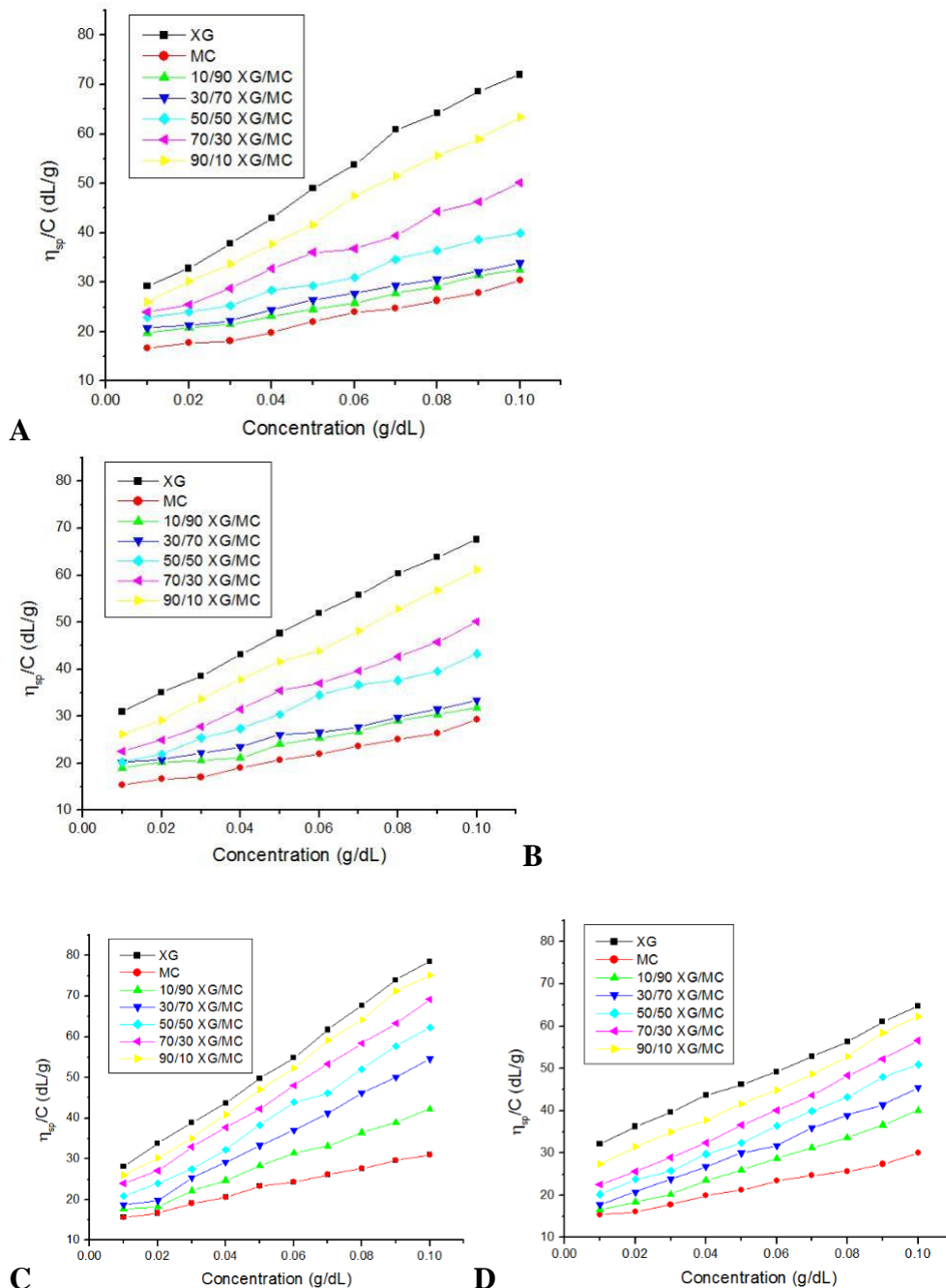


Figure 4: Huggins' plot for A) XG/MC blend at 30°C, XG/MC blend at 40°C, C) XG/MC blend – 0.02 wt% maghemite nanocomposite at 30°C, and D) XG/MC blend – 0.02 wt% maghemite nanocomposite at 40°C.

Table 1: Slope values from Huggins plots

Composition (XG/MC)	Blends		Blend – 0.02 wt% maghemite composites	
	30°C	40°C	30°C	40°C
0/100	153.290	151.139	175.684	161.654
10/90	146.927	150.169	282.642	261.533
30/70	151.884	148.030	411.581	301.703
50/50	201.012	256.945	472.787	344.375
70/30	290.212	298.993	508.836	379.460
90/10	420.115	386.418	566.400	380.339
100/0	500.812	414.054	568.272	351.836

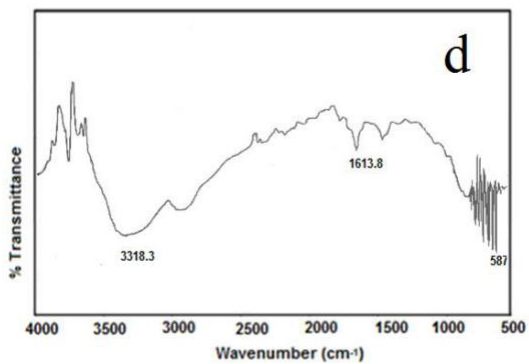
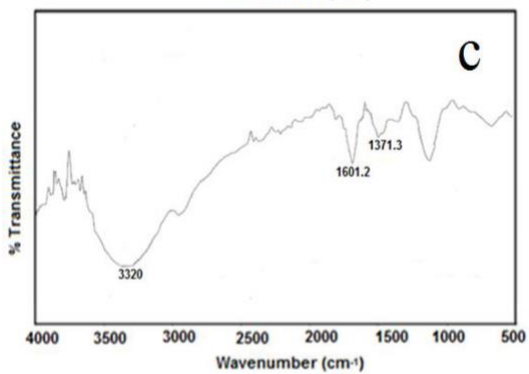
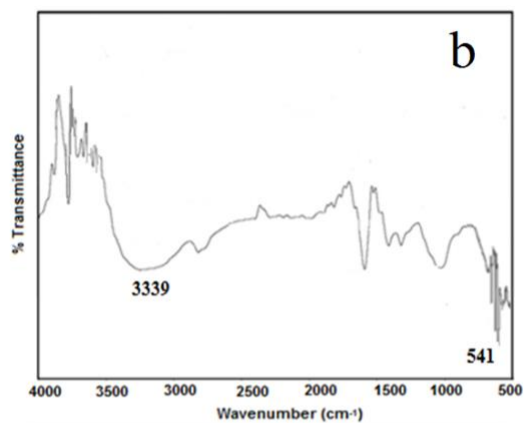
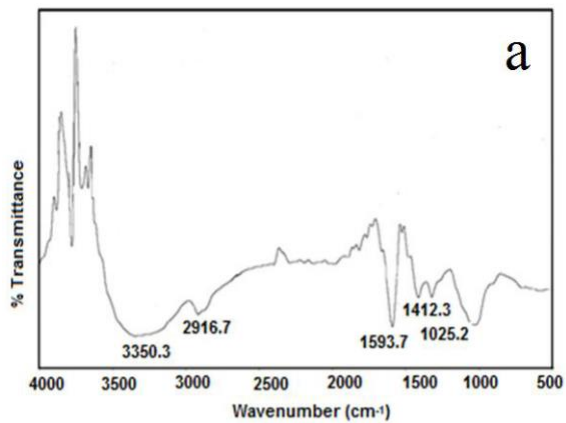
The plots were linear for XG, XG - 0.02 wt% maghemite nanocomposite, MC, MC - 0.02 wt% maghemite nanocomposite, blends of XG/MC, and blend – 0.02 wt% maghemite nanocomposites. All the plots of blends with 0.02 wt% maghemite showed higher slope variation confirming the miscibility. Whereas for blends without maghemite nanoparticles higher slope variation is observed for 50/50, 70/30, and 90/10 blend composition. Without the presence of maghemite nanoparticles the XG/MC blend is miscible only when the XG content is 50% or more in the blend.

3.5 Fourier transform infrared spectroscopic measurements

FTIR spectra of XG, XG – 0.02 wt% maghemite composite, MC, MC – 0.02 wt% maghemite composite, and their blend films (50/50) were recorded. Figure 6 shows, the FTIR spectra of pure and blend films in the wavelength range of 4000-500 cm^{-1} . The FTIR spectra of MC (Figure 5b) showed a hydroxyl group (–OH stretching) at 3350.3 cm^{-1} , and 1593.7 cm^{-1} is due the –OH bond belonging to water molecules, a hydrocarbon group (C-H stretching of the –CH₂ groups) at 2916.7 cm^{-1} , a –CH₂ scissoring around 1412 cm^{-1} and O- stretching at 1026 cm^{-1} [24, 25].

On the other hand, the bands of XG (Figure 5c) appeared at 3320.0 cm^{-1} for the hydroxyl groups and at 1601.2 cm^{-1} and 1371.3 cm^{-1} for the asymmetric –COO[–] stretching vibration and symmetric –COO[–] stretching vibrations of pyruvate and glucuronate groups respectively [26].

The spectrum of the XG/MC blend film was characterized by the presence of the absorption bands typical to that of the pure components, with the intensity roughly proportional to the blending ratio. In the case of 50/50 XG/MC and 50/50 XG/MC blend – maghemite nanocomposite, the asymmetric –COO[–] stretching vibration and symmetric –COO[–] stretching vibrations of pyruvate and glucuronate groups shifted to 1598.2 cm^{-1} , 1405.8 cm^{-1} and 1596.4 cm^{-1} , 1405.6 cm^{-1} respectively (Figure 5e, 5f). It is noticed that the hydroxyl stretching bands became much broader with increasing MC content. The results confirm [27] the presence of hydrogen bonding between the hydroxyl groups of MC and carbonyl groups of XG.



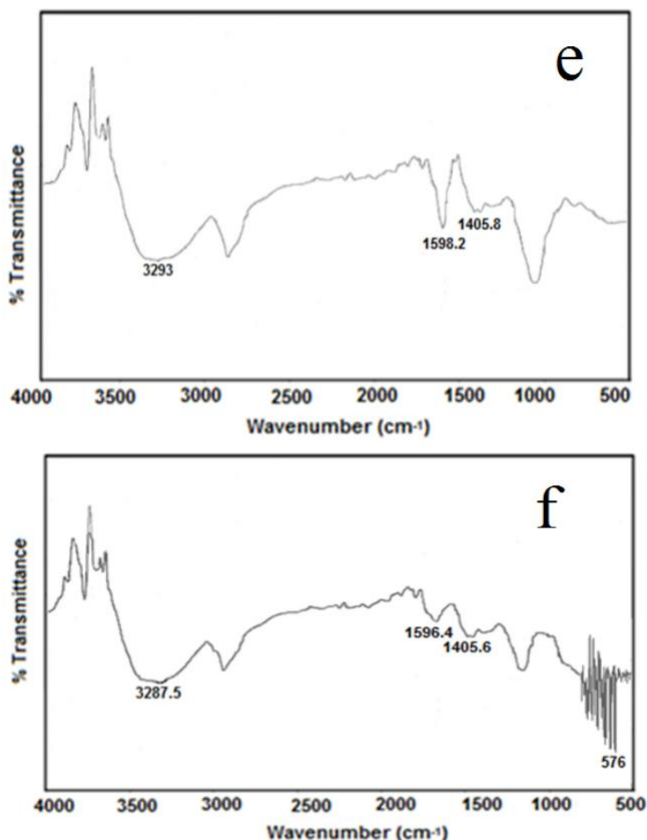
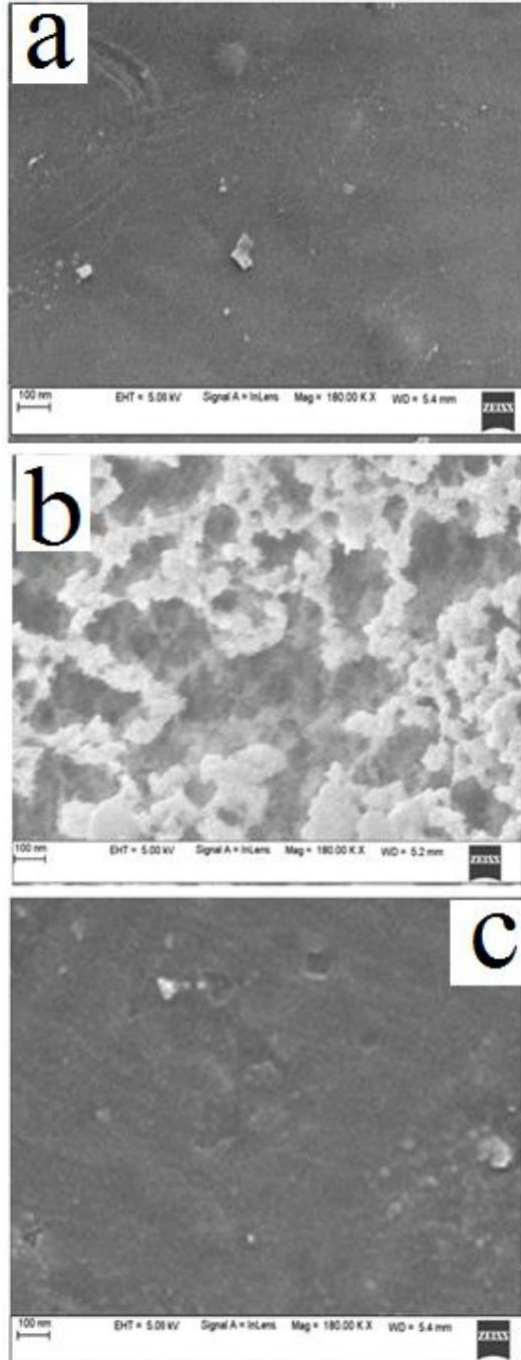


Figure 5: FTIR spectra of a) MC, b) MC – maghemite nanocomposite, c) XG, d) XG – maghemite nanocomposite, e) 50/50 XG/MC blend, and f) XG/MC – maghemite nanocomposite

3.6 Morphological studies

All the solution-casted films of XG, XG – maghemite nanocomposite, MC, MC – maghemite nanocomposite and their blend films (50/50) were characterized by SEM to check the morphology of the blends/nanocomposites. The results are given in Figure 6.



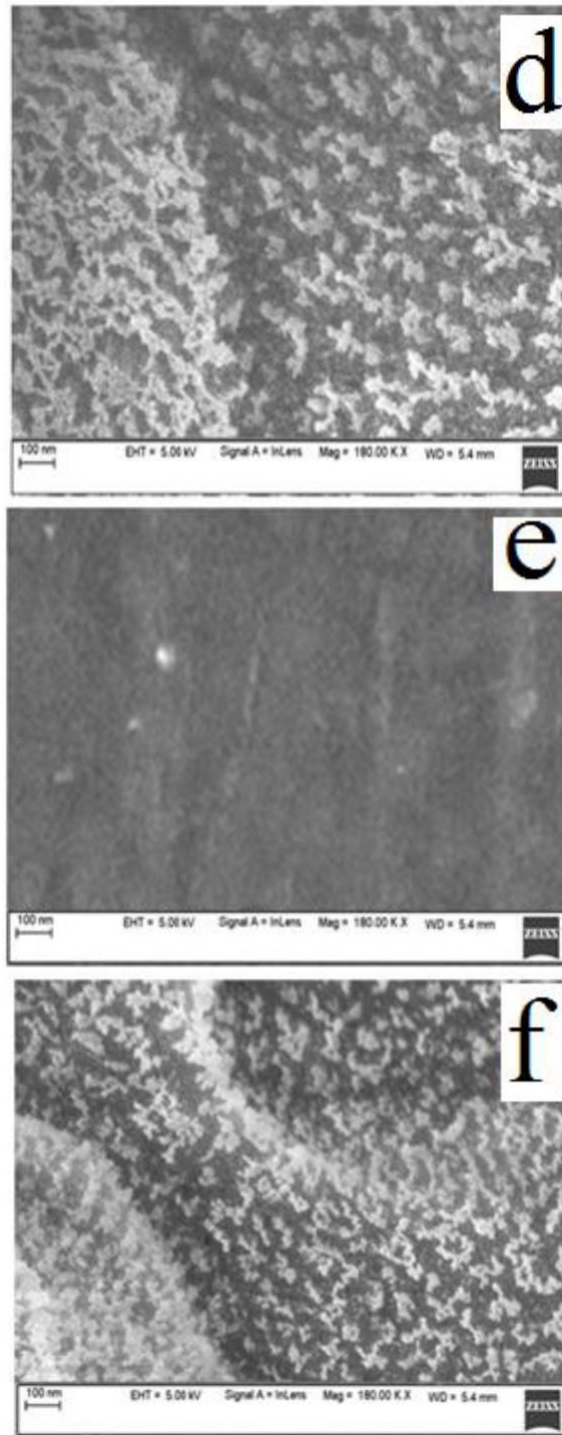


Figure 6: SEM micrographs for a) MC, b) MC – maghemite nanocomposite, c) XG, d) XG – maghemite nanocomposite, e) 50/50 XG/MC blend, and f) 50/50 XG/MC blend – maghemite nanocomposite

50/50 XG/MC blend (Figure 6e) did not show any aggregated particles and it can be observed that the MC granule was well distributed in the XG matrix, confirming a good interaction between XG and MC. It was distinctly observed that the blend is homogeneous, and displayed in the form of a sandwich, which

suggests that these blends were miscible [27]. The XG – maghemite nanocomposite (Figure 6d) and 50/50 XG/MC blend – maghemite nanocomposite (Figure 6f) shows the uniform distribution of maghemite nanoparticles.

3.7 Thermogravimetric analysis

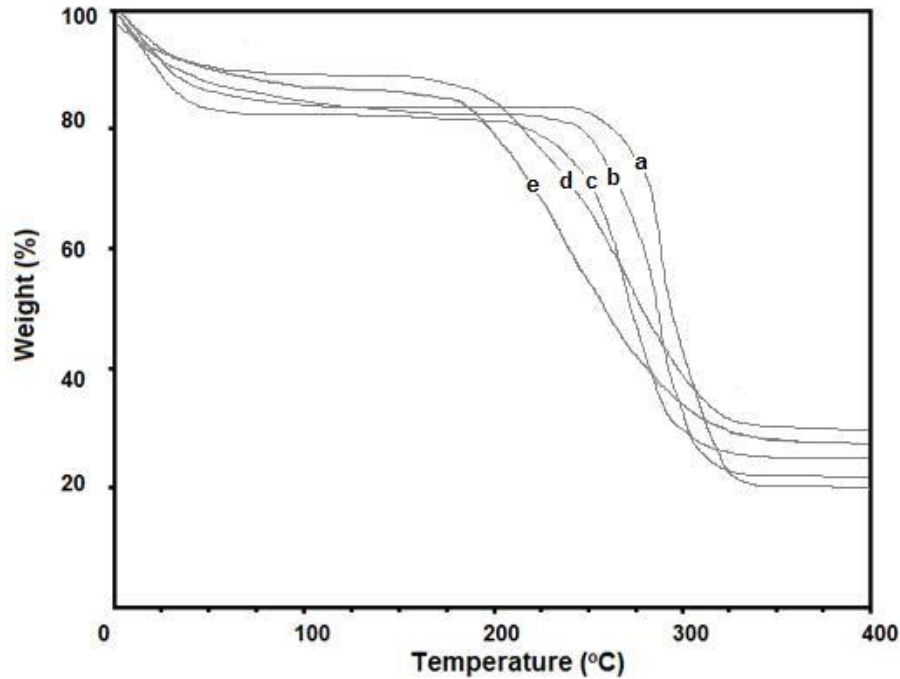


Figure 7: TGA curves of a) XG, b) 90/10 XG/MC, c) 70/30 XG/MC, d) 50/50 XG/MC, and e) MC

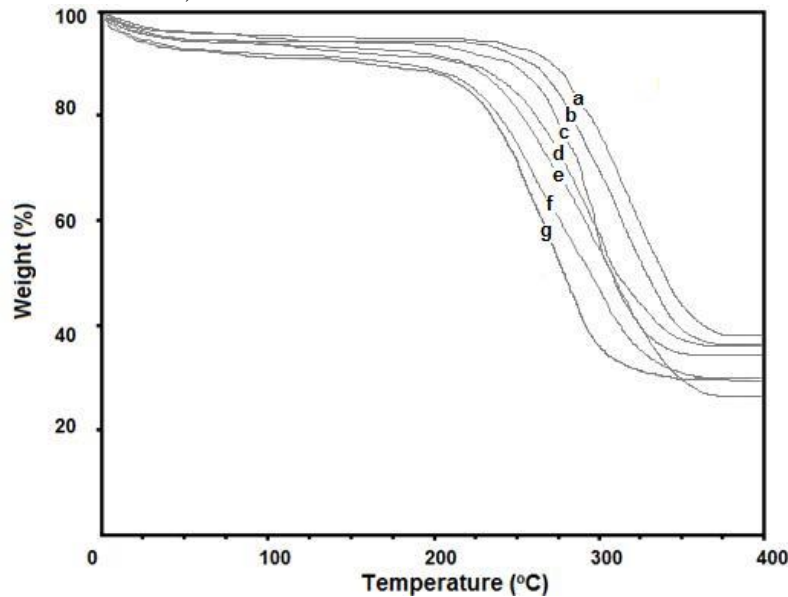


Figure 8: TGA curves of composites of 0.02 wt% maghemite with a) XG, b) 90/10 XG/MC, c) 70/30 XG/MC, d) 50/50 XG/MC, e) 30/70 XG/MC, f) 10/90 XG/MC, and g) MC

Table 2: Parameters evaluated from the thermograms of XG, MC, XG/MC blends and their maghemite composites

Composition		Temperature at different weight loss ($\pm 0.5^\circ\text{C}$)					
		T ₀	T ₂₀	T ₄₀	T ₅₀	T ₆₀	T _{max}
GG/HPMC blends	0/100	184	199	240	256	285	305
	50/50	187	215	261	277	297	329
	70/30	206	222	264	272	281	313
	90/10	230	247	278	284	295	318
	100/0	244	263	289	293	303	351
blend GG/HPMC maghemite composites	0/100	203	235	264	277	301	318
	10/90	199	237	276	294	313	331
	30/70	204	253	291	309	321	335
	50/50	214	261	296	310	336	355
	70/30	227	274	299	311	339	359
	90/10	247	282	315	328	348	364
	100/0	271	293	324	337	365	375

The samples of XG, XG – maghemite nanocomposite, MC, MC – maghemite nanocomposite, XG/MC blends (90/10, 70/30, and 50/50) and XG/MC blend – maghemite nanocomposite were characterized by thermogravimetric analyzer under nitrogen environment (Figure 7, and 8). TG curve shows that the samples have two degradation stages - the first stage is the water loss of films and the second stage which includes the depolymerisation, cellulose ethers degradation, decomposition (thermal and oxidative), steaming, and disposal of volatile compounds [28].

The temperature characteristics are calculated and shown in Table 2. The thermal characteristics of the blend compositions showed composition dependency. Addition of maghemite nanoparticle improved the thermal stability of the pure polymers and the blends. The blend – composites showed composition depended thermal properties confirming intermolecular interaction between the polymers.

3.8 Tensile strength measurements

XG/MC blends showed composition dependent tensile properties (Table 3). 90/10, 70/30 XG/MC blend – 0.02 wt% maghemite composites also showed improved composition dependent tensile properties.

Table 3: Tensile strength at yield, % of elongation and tensile modulus of XG, MC, and XG/MC blends and their wt% maghemite composites

Composition		Tensile Strength at Yield (MPa)	% Elongation	Tensile Modulus (MPa)
XG/MC blends	0/100	38.21	10.74	978.6
	70/30	32.4	7.12	722.4
	90/10	29.7	6.45	689.8
	100/0	27.4	6.12	647.3
XG/MC blend/maghemite composites	0/100	36.5	9.54	945.8
	10/90	33.1	8.88	726.5
	30/70	32.5	7.56	682.6
	50/50	31.2	6.55	645.4
	70/30	29.6	6.21	602.3
	90/10	28.7	5.87	596.6
	100/0	26.8	5.48	587.8

5. Conclusion

Based on viscosity, ultrasonic velocity, density and refractive index measurements, it is found that the polymer blend of XG/MC blend is miscible when XG content is 50% and more in the blend. The variation of temperature did not have any significant effect on the miscibility. The morphology, thermal and mechanical properties were analysed using SEM, TGA, and tensile strength measurement techniques. The effect of 0.02 wt% maghemite on the properties of XG, MC, and their blends studies and showed that 0.02 wt% maghemite compatibilizes the XG/MC blends.

6. Acknowledgement

The co-author, P. Prasad acknowledges the financial support provided by VGST (CISEE - GRD No. 538), Govt. of Karnataka, India for the purchase of some of the instruments used to carry out the research work.

References

- V. Rao, P. V. Ashokan and M. H. Shridhar, Miscible blends of cellulose acetate hydrogen phthalate and PVP characterization by viscometry, ultrasound and DSC, J. Appl. Polym. Sci., 76, 859-867, 2000.
- Changhua Liu, Chaobo Xiao and Hui Liang, Properties and structure of PVP - Lignin blend films, J. Appl. Polym. Sci., 95, 1405-1411, 2005.
- S. A. Jones, G. P. Martin, P. G. Royall and M. B. Brown, Biocompatible polymer blends: Effects of physical processing on the molecular interaction of PVA and PVP, J. Appl. Polym. Sci., 98, 2290-2299, 2005.

- Wei-Chi Lai and Wen-Bin Liau, Study of the miscibility and crystallization behaviour of PEO/PVA blends, *J.Appli.Polym. Sci.*, 92, 1562-1568, 2004.
- Yasuyuki Agari, Kiyofumi Sakai, Yosikazu Kano and Ryoki Nomura, Preparation and properties of the biodegradable graded blend of poly (L-lactic acid) and poly (ethylene oxide), *J. Polym. Sci., Part: B Polymer Physics*, 45, 2972-2981, 2007.
- Jao D, Mou X, Hu X. Tissue Regeneration: A Silk Road. *J Funct Biomaterials*. 2016;7(3):22.
- M. Swietek, W. Tokarz, J. Tarasiuk, S. Wronski, M. Blazewicz, Magnetic Polymer Nanocomposite for Medical Application, *Acta Physica Polonica A*, 125 (4), 2014, 891-894.
- N. Bock, A. Riminucci, C. Dionigi, A. Russo, A. Tampieri, E. Landi, V.A. Goranov, M. Marcacci, V. Dediu, *Acta Biomater.* 6, 786, (2010).
- Abd Elrahman, A. A., Mansour, F. R. (2019). Targeted magnetic iron oxide nanoparticles: Preparation, functionalization and biomedical application. *J. Drug Deliv. Sci. Technol.*, 52, 702–712.
- Xu, C., Akakuru, O. U., Zheng, J. J., Wu, A. G. (2019). Applications of iron oxide-based magnetic nanoparticles in the diagnosis and treatment of bacterial infections. *Front. Bioeng. Biotechnol.*, 7, 141.
- M. S. Bhavya, K. S. Sudhanva Narayana, M. B. Savitha, P. Prasad, Guar gum (GG)/methylcellulose (MC) blends and their composites with maghemite nanoparticles, *International Journal of Management and Humanities*, 4(9), 96-102, 2020
- Bhavya M. S., Sudhanva Narayana K. S., Savitha M. B., Prasad P., Biocompatible Maghemite Nanoparticles Compatibilization of GG/CMC Blends in Aqueous Solution, *International Journal of Applied Engineering and Management*, 4 (1), 184-190, 2020.
- Bhavya M. S., Athira Lakshmanan P., Sudhanva Narayana K. S., Savitha M. B., Prasad P., Investigation on γ -Fe₂O₃ Nanoparticles Compatibilization on Guar Gum/Poly(vinyl alcohol) Blends, *International Journal of Applied Engineering and Management*, 4(1), 219-225, 2020.
- G.S. Guru, P. Prasad, H.R. Shivakumar, S. K. Rai, Miscibility Studies of Polysaccharide Xanthan Gum/PVP Blend, *Journal of Polymers and the Environment*, 18 (2), 135-140, 2010.
- P. Prasad, G. S. Guru, H. R. Shivakumar, K. Sheshappa Rai, Miscibility, Thermal, and Mechanical Studies of Hydroxypropyl Methylcellulose/Pullulan Blends, *Journal of Applied Polymer Science*, 110 (1), 444-452, 2008.
- G.S. Guru, P. Prasad, H.R. Shivakumar, S. K. Rai, Studies on the Compatibility of Pullulan – Carboxymethyl Cellulose Blend Using Simple Techniques, *Malaysian Polymer Journal*, 3 (2), 13-23, 2008.
- G.S. Guru, P. Prasad, H.R. Shivakumar, S. K. Rai, Miscibility and thermal studies of PVP/Pullulan blends, *International Journal of Plastics Technology*, 14 (2), 234-245, 2010.

- [18] Vishwanath Bhat, H. R Shivakumar, Rai K. Sheshappa, Sanjeev Ganesh, P. Prasad, G. S. Guru, B. B. Bhavya, Miscibility and Thermal Behavior of Pullulan/Polyacrylamide Blends, *Journal of Macromolecular Science, Part A*, 48 (11), 920-926, 2011.
- P. Prasad, G. S. Guru, H. R. Shivakumar, K. Sheshappa Rai, Investigation on Miscibility of Sodium Alginate/Pullulan Blends, *Journal of Polymers and the Environment*, 20 (3), 887-893, 2012.
- G.S. Guru, P. Prasad, H.R. Shivakumar, S. K. Rai, Miscibility, thermal, and mechanical studies of methylcellulose/poly(vinyl alcohol) blends, *International Journal of Research in Pharmaceutical Chemistry*, 2 (4), 957-968, 2012.
- Bhavya, B. B.; Shivakumar, H. R.; Vishwanath Bhat; Prasad, P.; Guru, G. S., Investigation of miscibility of biocompatible guar gum/pullulan polymer blend, *Malaysian Polymer Journal*, 8 (1), 33-37, 2013.
- Bhavya M. S., Savitha M. B., Prasad P., Miscibility studies of GG/CMC blends in aqueous solution, *International Journal of Advance Research in Science and Engineering*, 6 (1), 514-523, 2017.
- Prasad P., Bhavya M. S., Abhijith P. P., Sreelakshmi S. K., Savitha M. B., Miscibility studies of GG/PVA blends in aqueous solution, *International Journal of Advance Research in Science and Engineering*, 6 (9), 1-8, 2017.
- Reshmi G, Kumar PM, Malathi M. Preparation, characterization and dielectric studies on carbonyl iron/cellulose acetate hydrogen phthalate core/shell nanoparticles for drug delivery applications. *Int J Pharm* 2009;365:131–5.
- Arias JL, Lopez-Viota M, Ruiz MA, Lopez-Viota J, Delgado AV. Development of carbonyl iron/ethylcellulose core/shell nanoparticles for biomedical applications. *Int J Pharm* 2007;339:237–45.
- Lang, C., Schuler, D., Faivre, D. (2007). Synthesis of magnetite nanoparticles for bio- and nanotechnology: Genetic engineering and biomimetics of bacterial magnetosomes. *Macromol. Biosci.*, 7, 144-151.
- Prasad P., Bhavya M. S., Nagesh Bhat, Momin Ashraf, Krishnaraja Acharya, Savitha M. B., Physico-chemical and thermal property studies of GG/PVA blend thin films, *International Journal of Advance Research in Science and Engineering*, 7 (1), 1-7, 2018.
- Prasad P., Bhavya M. S., Abhijith P. P., Sreelakshmi S. K., Savitha M. B., Physico-chemical and thermal property studies of GG/CMC blend thin films, *International Journal of Advance Research in Science and Engineering*, 6 (6), 572-578, 2017.